# Ultrasonographic evaluation of the thorax in dogs with tick paralysis

## Evaluación ecográfica del tórax en perros con parálisis por garrapatas

*Erdem Gülersoy\** , *Canberk Balıkçı* , *İsmail Günal* , *Adem Şahan* , *Esma Kısmet*

*Harran University, Veterinary Faculty, Department of Internal Medicine. Şanlıurfa, Türkiye.*
*Corresponding author: egulersoy@harran.edu.tr*

## ABSTRACT

Tick paralysis is a rapidly progressing motor paralysis caused by a neurotoxin in the saliva of certain tick species. Delayed diagnosis can lead to increased mortality due to respiratory failure. Thus, the aim of this study is to describe thoracic ultrasonography lesions in dogs with tick paralysis and to identify potential patterns that could aid in diagnosis and prognosis prediction. The animal material consisted of 58 dogs in total, 10 of which were healthy and 48 of which were suspected to be affected by tick paralysis. Clinical, laboratory and thoracic ultrasonographic examinations were performed. Expiratory dyspnea with sinus tachycardia; fine crackles, polyphonic wheezing, and pleural rub on lung auscultation were observed in the tick–paralyzed dogs. The most common abnormal thoracic ultrasonography patterns were, in order of prevalence: B–lines > 3, wet lung, pulmonary nodule, confluent B–lines, loss of A–lines, consolidation, fibrosis, and isolated B–lines. In addition, the pleural thickness of the tick–paralyzed dogs was higher than that of the healthy ones. Among these findings, B–lines > 3 were interpreted as indicative of possible pulmonary parenchymal damage, while the loss of A–lines was attributed to decreased aeration. The presence of pulmonary nodule and fibrosis might be due to bronchopneumonia and aspiration pneumonia due to regurgitation. The wet lung pattern was associated with a predisposition to lung congestion. It was concluded that recognizing thoracic ultrasonography findings may assist in identifying the presence and grading the extent of lung damage, as well as determining the necessity of lung decongestion treatment in tick paralysis cases.

**Key words:** B–lines; dog; pleural thickness; wet lung; thoracic ultrasonography

## RESUMEN

La parálisis por garrapatas es una parálisis motora de rápida progresión causada por una neurotoxina en la saliva de ciertas especies de garrapatas. Un diagnóstico tardío puede llevar a un aumento en la mortalidad debido a insuficiencia respiratoria. Por lo tanto, el objetivo de este estudio fue describir las lesiones detectadas mediante ecografía torácica en perros con parálisis por garrapatas e identificar patrones potenciales que puedan ayudar en el diagnóstico y la predicción del pronóstico. El material animal consistió en un total de 58 perros, 10 de los cuales estaban sanos y 48 se sospechaba que estaban afectados por parálisis por garrapatas. Se realizaron exámenes clínicos, de laboratorio y ecográficos torácicos. Se observó disnea espiratoria con taquicardia sinusal; estertores finos, sibilancias polifónicas y roce pleural en la auscultación pulmonar de los perros paralizados por garrapatas. Los patrones anormales más comunes en la ecografía torácica fueron, en orden de prevalencia: líneas B > 3, pulmón húmedo, nódulo pulmonar, líneas B confluyentes, pérdida de líneas A, consolidación, fibrosis y líneas B aisladas. Además, el grosor pleural de los perros con parálisis por garrapatas fue mayor que el de los sanos. Entre estos hallazgos, las líneas B > 3 se interpretaron como indicativas de posible daño parenquimatoso pulmonar, mientras que la pérdida de líneas A se atribuyó a una disminución de la aireación. La presencia de nódulo pulmonar y fibrosis podría deberse a bronconeumonía y neumonía por aspiración debido a regurgitación. El patrón de pulmón húmedo se asoció con una predisposición a la congestión pulmonar. Se concluyó que el reconocimiento de los hallazgos ecográficos torácicos puede ayudar a identificar la presencia y a clasificar la extensión del daño pulmonar, así como a determinar la necesidad de tratamiento de descongestión pulmonar en casos de parálisis por garrapatas.

**Palabras clave:** Líneas B; perro; grosor pleural; pulmón húmedo; ecografía torácica

## INTRODUCTION

Tick paralysis, a case of acute flaccid paralysis characterized by vomiting, regurgitation and sudden onset of lower motor neuron weakness and respiratory failure in severe cases, is a significant veterinary problem in certain parts of the world [1]. A wide variety of domestic animals are affected, including horses, cattle, dogs, cats, sheep, and poultry [2]. After attaching to the host, ticks typically undergo a latent period of 3-6 days (d), during which they engorge and their salivary glands enlarge, producing a neurotoxin. Paralysis signs usually result from the engorgement of a single tick, although multiple ticks may also contribute, and occasionally, no tick is found [3]. Early clinical signs typically include hind limb ataxia, which often progresses to quadriplegia [4]. In addition to the non–specific clinical findings observed in tick paralysis cases, mortality rates can reach up to 100% in untreated cases due to complications involving the cardiovascular, gastrointestinal, and respiratory systems. The major clinical abnormality and cause of mortality in tick paralysis cases is respiratory failure [5]. Current hypotheses explaining the development of respiratory failure in tick paralysis involve neuromuscular blockade of respiratory muscles, potentially leading to hypoventilation. This effect may be exacerbated by central respiratory depression. Additionally, paralysis of the pharynx and larynx can result in upper airway obstruction, while pulmonary parenchymal disease may also contribute [6]. Pulmonary parenchymal disease in tick paralysis is commonly linked to cardiogenic pulmonary edema resulting from the tick's salivary toxin. Aspiration pneumonia is a common complication in patients with tick paralysis–related lung disease. It is related to dysfunction of the esophagus, pharynx, and larynx, all of which are frequently observed in patients with tick paralysis [2, 7].

During the last decade, thoracic ultrasonography has seen increased use as both a diagnostic and monitoring tool. Previous descriptions have detailed the identification of lung consolidations on thoracic ultrasonography, characterized by either a tissue sign involving the full width of the lung lobe or a shred sign affecting part of the lung lobe's width, along with an increased number of B–lines and the presence of pleural effusion [8, 9]. In Veterinary Medicine, point–of–care (POC) thoracic ultrasonography has been used to identify pulmonary hemorrhage, congestive heart failure, and alternative causes of alveolar–interstitial syndrome [10]. Thoracic ultrasonography has shown promising diagnostic performance in critically ill patients experiencing respiratory failure from various causes. It was reported that it offers more valuable clinical insights compared to physical examination and bedside radiography [11, 12]. Nevertheless, there is currently no study examining thoracic ultrasonography findings in dogs with acute flaccid paralysis due to tick paralysis.

Discerning the primary pathological processes is essential for guiding treatment and determining prognosis for patients. Managing clinical cases related to pulmonary disease poses significant challenges for veterinarians and often carries a poor prognosis. Therefore, early recognition of pulmonary edema and parenchymal disease is crucial for improving survival rates. Considering that the leading cause of mortality in tick paralysis cases are respiratory abnormalities such as pulmonary edema, aspiration pneumonia and respiratory failure, the purpose of this study is to describe thoracic ultrasonography lesions in dogs with tick paralysis and to identify patterns that may aid in diagnosis, treatment planning, and prognosis prediction.

## MATERIALS AND METHODS

This study received approval from the Local Ethics Committee for Animal Experiments at Harran University on 09/05/2022 with session 2022/003 and decision number 01-06. All animal owners gave their consent for participation in the study.

### Animals

The Patient group for this study consisted of 48 dogs (_Canis lupus familiaris_), each displaying symptoms indicative of acute flaccid paralysis, including anorexia, regurgitation, ataxia, abnormal vocalization, and weakness in standing, and all were found to have ticks upon examination. The Healthy group comprised 10 clinically healthy dogs admitted for vaccination and/or check–up purposes. All animals were admitted to the animal hospital of Veterinary Faculty, Harran University.

### Inclusion/Exclusion Criteria and Forming Groups

The inclusion criteria for the tick–paralyzed dogs required that dogs have no history of prior diseases other than tick paralysis—including respiratory, cardiovascular, or gastrointestinal disorders that could cause vomiting, diarrhea, anorexia, labored breathing, or rapid fatigability—have not been treated with antiparasitic medication within the past month, and exhibit signs of acute flaccid paralysis. The accepted clinical findings for acute flaccid paralysis include sudden onset weakness that intensifies within a few days, characterized by weakness in respiratory muscles and swallowing ability. Additionally, there is typically an absence of spasticity, hyperreflexia, clonus, extensor plantar reflexes, and muscle contraction due to impairment of motor pathways extending from the cortex to muscle fibers [13].

The primary differential diagnosis for the clinical manifestations observed in the dogs included in the study and suspected of tick paralysis involved considering common lower motor neuron conditions in dogs, including botulism, acute idiopathic polyneuropathy, and snake envenomation [14]. In summary, botulism can occur in dogs following the consumption of rotten food or carcasses; however, this was not the case for the dogs described here, as they are solely fed commercial dry dog food. Clinically, it is marked by difficulties in grasping and swallowing food, along with drooling. Acute idiopathic polyneuropathy has been observed in dogs that have come into contact with raccoon saliva or have a history of systemic illness. It is characterized by hyperesthesia and neurogenic muscle atrophy enduring for over five to seven days [3, 14]. Although acute idiopathic polyradiculoneuritis can involve the cranial nerves and result in partial or complete respiratory paralysis due to the involvement of intercostal or phrenic nerves, the majority of clinical symptoms are usually limited to the limbs [15]. Typically, the respiratory pattern in the neuromuscular paralysis conditions mentioned is rapid and shallow. In contrast, the present cases exhibited a slow respiratory pattern with a notable expiratory effort, resembling what is seen in tick paralysis [3]. Myopathy was also excluded, as it is manifests as proximal weakness or fatigue, preserved sensitivity, and followed by a loss of reflexes, typically following significant atrophy [16]. While the neurological manifestations discussed here share similarities with those of other lower motor neuron diseases, they closely resemble the findings typically associated with tick paralysis [17], the cases

were validated by the quick improvement (median: 26 hours (h), min: 16 h, max: 35 h) observed after acaricidal treatment and tick removal [14]. Hence, the neurological symptoms described here were differentiated from other common causes of lower motor neuron diseases that mimic tick paralysis. Dogs that did not exhibit this clinical presentation were excluded from the study. Also, dogs exhibiting signs of acute flaccid paralysis but with no ticks detected, those with a different etiology determined based on medical history, clinical evaluation, and laboratory tests, and those affected by other neurological diseases in dogs (such as spinal cord pressure, epidural abscesses, and exposure to toxic plants or snakes) were also excluded from the study. Moreover, 8 dogs were excluded from the study because they did not improve clinically despite acaricidal treatment and tick removal.

Consequently, dogs diagnosed with tick paralysis due to Rhipicephalus sanguineus (each collected tick was stored in separate vials and identified at the species level through morphological analysis) were confirmed through the ex juvantibus method [2, 7, 14], were included in the Patient group (n: 40). Dogs that did not have any history of disease and were deemed to be healthy as a result of physical, laboratory, radiographic and ultrasonographic examinations were included in the Healthy group (n: 10).

### Physical Examinations

Heart and respiratory rates, body temperature, heart and lung auscultation (using Littmann classic III stethoscope, 3M Health, Minnesota, USA), palpable lymph nodes and gingival capillary refill times (CRT) of all dogs were evaluated. Additionally, the body weight (using a digital veterinary scale, Lider Terazi, İstanbul, Türkiye) and body surface area (BSA) using the formula K × (body weight in grams$^{2/3}$) × $10^{-4}$, K = constant (10.1 for dogs) of each dog were calculated. The presence of ticks was assessed by manually counting them on various anatomical body parts including the head, ears, chest–neck, thorax, abdomen, front and hind legs, interdigital areas, axilla and tail, and the number of ticks was recorded.

### Laboratory Examinations

Venous blood samples (5-10 mL) were drawn from all dogs via cephalic vein puncture, ensuring minimal stress. Complete blood count (CBC) was performed from blood samples which were transferred to Ethylenediaminetetraacetic acid (EDTA) tubes within 15 min (using and autoanalyzer, Sysmex pocH-100i, Japan). Within the scope of CBC, leukocyte count, lymphocyte count, granulocyte count, monocyte count, red blood cell count (RBC), mean corpuscular volume (MCV), hematocrit, mean corpuscular hemoglobin (MCH), mean corpuscular hemoglobin concentration (MCHC), red cell distribution width (RDW) and hemoglobin were evaluated. The leftover sample was used for microscopic blood smear examinations, which included blood and buffy coat smears for _Anaplasma platys, Ehrlichia canis, Babesia_ spp., and _Hepatozoon canis_. Each smear was examined using a light microscope (with Diff–quik staining and oil immersion, 1000x magnification, Olympus 2-U050H2 light microscope, Tokyo, Japan).

### Thoracic radiography

To investigate the presence of any concomitant disorders, such as cardiomegaly, masses, pneumothorax, or effusions, thoracic radiographs were performed as part of the inclusion/exclusion criteria verification. Each thoracic radiographic examination included three projections: right and left lateral images, as well as both ventrodorsal (VD) and dorsoventral (DV) images, using the Fujifilm Veterinary CR X–ray System, Prima II, Tokyo, Japan.

### Thoracic ultrasonography

Thoracic ultrasonographic examinations were conducted on all dogs of the present study. The examinations were performed with the dogs in a standing or sternal position, using a microconvex probe (5-8 MHz, 6C2P transducer, Mindray Z60, Shenzhen, China). Prior to the examination, an appropriate amount of alcohol and/ or gel was applied to the area without shaving it. All animals were assessed with a single portable ultrasound machine (Mindray Z60, Shenzhen, China), and the depth was adjusted to suit the clinician's preferences for each individual animal. To visualize the gator sign, which includes the pleural line and two ribs, the transducer was placed in a transverse position relative to the ribs. Four regions were examined on each thoracic side (caudodorsal, perihilar, middle, and cranial) with one scan for each region [18]. The presence of A–lines accompanied by lung sliding was interpreted as indicative of a normally aerated lung. B–lines were used to recognize interstitial–alveolar edema. The occurrence of B–lines was classified according to a 5-point scale. The shred sign indicates partial lung consolidation, characterized by a deeper border of consolidated lung tissue that appears shredded and irregular where it connects with the aerated lung. The tissue–like sign manifests when lung tissue resembles that of the liver, which is caused by translobar consolidation. The pulmonary nodule sign indicates a well–circumscribed area fully enveloped by aerated lung. B–lines project from the distal border of each consolidation type downward on the screen. According to earlier studies in human medicine, additional ultrasound abnormalities were described, including the shred sign, tissue–like sign, and nodule sign [19, 20].

### Statistical analysis

Data analysis was conducted with SPSS 25.00 (SPSS for Windows®) statistical software, employing the one–sample Kolmogorov–Smirnov test to assess whether the data were parametric or non–parametric. Non–parametric data were evaluated as median (min, max) using Mann–Whitney U, Kruskal–Wallis test. Statistical significance was regarded as _P_<0.05.

## RESULTS AND DISCUSSION

### Animals

All dogs included in the study were owned and fed commercial dry dog food. It was learned that the dogs of the Patient group were outdoor (31; 77.5%) or were taken outside twice a day for the toilet (9; 22.5%). 22 were male, 18 were female and the majority were mixbreed. The Healthy group comprised 4 male and 6 female mixed–breed dogs. Anamnestic data revealed that all dogs included in the study had no previous history of disease. Some had been vaccinated once (16; 40%), some twice (11; 27.5%), and the remaining dogs had not been vaccinated at all (13; 32.5%).

## Physical Examinations

The symptom duration of the tick–paralyzed dogs was 6 (4-11) d. The majority of the detected ticks {median: 39 (13-110)} were on the head, ears, chest–neck and less commonly on the tail base, respectively. The most common findings reported by the owners were difficulty standing (20; 50%) and ataxia (13; 32.5%). No abnormalities in terms of temperature, pain, or swelling were detected in the palpable lymph nodes of dogs with tick paralysis. Conjunctival mucosa was normal in color. Expiratory dyspnea was evident in the dogs of the Patient group (30; 70%). Fine crackle (14, 35%), polyphonic wheezing (10; 26%) and pleural rub (16; 40%) were determined as the most common abnormal sounds in lung auscultation. Auscultation of the heart revealed no abnormalities other than sinus tachycardia (26; 65%). Additionally, during the clinical examination, more ticks were removed from the dogs, and all were treated with a spot–on formulation containing 10% Fipronil and 9% (S)–Methoprene (Frontline Combo, Merial S.A.S., France). Rectal body temperature and respiratory and heart rates were higher in the Patient group dogs than in the Healthy group dogs ($P<0.0001$). Physical examination findings are presented in Supplementary file (TABLE I).

**TABLE I**
**Physical examination findings**

| Parameters | Patient group, n:40 median (min–max) | Healthy group, n:10 median (min–max) | *P*–value |
|---|---|---|---|
| Body weight (kg) | 7.3 (6-17.1) | 9.45 (4.2-16.7) | 0.3510 |
| BSA (m$^2$) | 0.37 (0.25-0.67) | 0.45 (0.25-0.64) | 0.4620 |
| Heart rate (beats/min) | 101.5 (68-144) | 78 (65-96) | 0.0001 |
| Body temperature (°C) | 39.1 (36.6-40) | 38.1 (37.7-38.5) | 0.0001 |
| Respiratory rate (breaths/min) | 82 (44-99) | 35 (24-46) | 0.0001 |
| CRT (sec) | 3 (2-4) | 3 (2-3) | 0.0640 |

BSA: Body surface area, using the formula K × (body weight in grams$^{2/3}$) × 10$^{-4}$, K = constant (10.1 for dogs). CRT: Capillary refill time

## Complete blood count

The CBC analysis revealed no statistical difference in the comparison of the investigated parameters between the two groups. CBC findings are presented in Supplementary file (TABLE II).
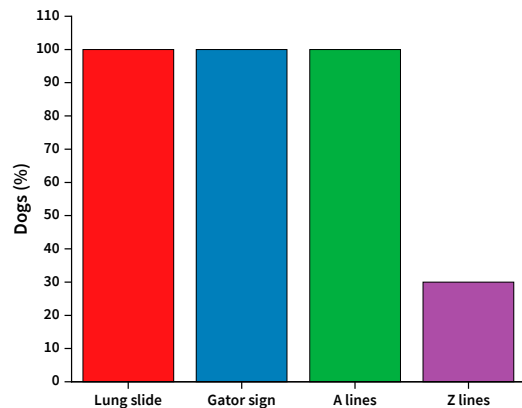
## Thoracic ultrasonography

As a result of the thoracic ultrasonographic examination of healthy dogs, lung slide, the gator sign, and A–lines were observed in all dogs (10, 100%). In addition to A lines in the Healthy group, Z lines were also detected in 3 dogs (30%). The distribution of thoracic ultrasonographic findings for the Healthy group is presented in FIG. 1A, and thoracic ultrasonographic images are presented in FIGS. 2, 3, 4 and 5. Thoracic ultrasonographic examination of the Patient group revealed that the most common abnormal findings were B–lines > 3 (8, 20%), wet lung (6, 15%), pulmonary nodule (6; 15%), thick pleura (6; 15%), confluent B–line (5; 12%), loss of A–line (3; 8%), consolidate (2; 5%), fibrosis

**TABLE II**
**Complete Blood Count findings**

| Parameters | Patient group, n:40 median (min-max) | Healthy group, n:10 median (min-max) | *P*–value |
|---|---|---|---|
| Leukocyte (×10$^9$·L$^{-1}$) | 11.01 (5.58-18.5) | 12.28 (6.12-15.17) | 0.7040 |
| Lymphocyte (×10$^9$·L$^{-1}$) | 3.82 (1.37-7.09) | 2.77 (1.8-7.4) | 0.6470 |
| Monocyte (×10$^9$·L$^{-1}$) | 1.25 (0.1-3.16) | 1.6 (0.29-3.3) | 0.5110 |
| Granulocyte (×10$^9$·L$^{-1}$) | 5.78 (1.33-13.4) | 4.32 (2.92-12.74) | 0.7330 |
| Erythrocyte (×10$^9$·L$^{-1}$) | 6.84 (5.13-8.83) | 7.25 (5.99-8.16) | 0.1580 |
| MCV (fL) | 65.35 (56-71.2) | 67.1 (54.5-79.3) | 0.3460 |
| Hematocrit (%) | 44.45 (34-60) | 47.5 (37-61) | 0.3720 |
| MCH (pg) | 22.12 (17.7-25.11) | 20.5 (17.5-24) | 0.1770 |
| MCHC (g·L$^{-1}$) | 31.35 (26.9-39.42) | 29.5 (28.9-33.4) | 0.1470 |
| RDW (fL) | 10.45 (8.26-14) | 11 (9.7-14.8) | 0.2720 |
| Hemoglobin (g·dL$^{-1}$) | 14.9 (11.2-19.7) | 14.9 (10.7-18.2) | 0.8760 |

MCV: Mean corpuscular volume, MCH: Mean corpuscular hemoglobin, MCHC: Mean corpuscular hemoglobin concentration, RDW: Erythrocyte distribution width



**A** Thoracic ultrasonographic examination findings in Healthy dogs

**B** Abnormal findings in Patient group
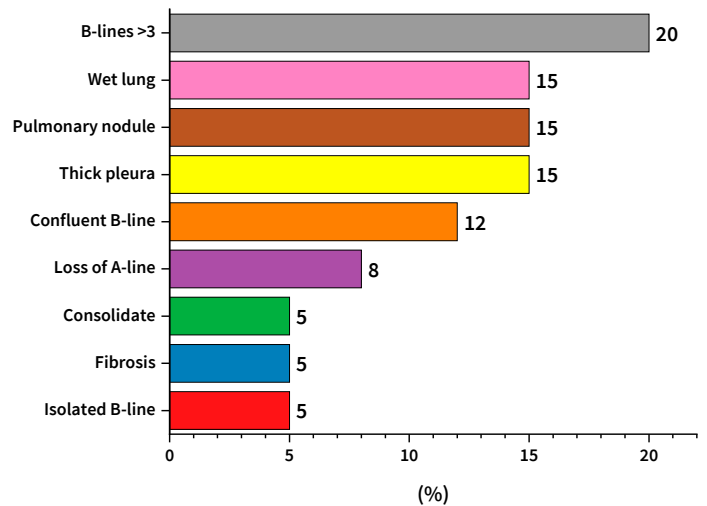
FIGURE 1. Distribution of thoracic ultrasonographic findings in the Healthy (A) and Patient (B) groups

(2; 5%) and isolated B–line (2; 5%). In addition, the pleural thickness of the tick–paralyzed dogs (median: 0.18 cm, minimum: 0.10, maximum: 0.24) was higher than that of the healthy ones (median: 0.10 cm, minimum: 0.08, maximum: 0.13) (*P*<0.0001). Distribution of thoracic ultrasonographic findings of dogs with tick paralysis are presented in FIG. 1B and thoracic ultrasonographic images are presented in FIGS. 6 to14.

Thoracic ultrasonography is a valuable and accessible diagnostic tool for assessing lower respiratory tract pathologies. Utilizing this technique is advisable in suspected cases of cardiogenic pulmonary edema, consolidation, atelectasis, embolism, neoplasia, pneumonia, pneumothorax, and interstitial lung diseases, particularly those with fibrosis. It is also beneficial for evaluating other lower respiratory tract signs, including dyspnea, pleural pain, fluid accumulation, and acute cough. This method is relatively inexpensive, non–ionizing, portable, and widely available. Moreover, it does not necessitate anesthesia or uncomfortable patient positioning, which is very important in critical care settings [19]. While respiratory failure was previously attributed solely to hypoventilation resulting from neuromuscular paralysis, recent pathogenesis studies in dogs affected by tick paralysis have highlighted the involvement of parenchymal disease and pulmonary edema. These findings suggest that hypoxemia may independently contribute to respiratory compromise in affected dogs. In cases of tick envenomation, respiratory decline is unique in that it may occur through one of two independent pathways: neuromuscular weakness (resulting in hypoventilation) or pulmonary disease (leading to hypoxemia) [5, 21]. As such, identifying the underlying pathophysiological process contributing to respiratory compromise in patients with tick paralysis can be crucial for determining tailored interventions and supportive treatments for each individual [22]. Therefore, the abnormal thoracic ultrasonography patterns detected in the present study, such as B–lines > 3, loss of A–lines, wet lung, and pulmonary nodule, may contribute to the development of individualized treatment protocols for dogs suffering from tick paralysis.

Comprising skin, subcutaneous fat, and muscle layers, the chest wall shows alternating patterns of hyper – and hypoechogenicity in the near field, immediately below the transducer. The parietal pleura lining the thoracic wall may not be distinctly visible; however, in a healthy dog, the visceral pleura and lung surface create a continuous echogenic line. Differentiation of the two pleural interfaces is possible through the gliding sign, with the hyperechoic pleuropulmonary interface gliding smoothly against the parietal pleura of the chest wall during breathing [23]. This sign is absent in conditions where the two pleural layers are not in contact with each other, such as in pneumothorax or pleural effusion. Correspondingly, it is not detected when the pleura are closely adhered to each other, as seen in pneumonia complicated by adhesions, pleurodesis, or in situations of absent respiration [24, 25].

Previous reports indicate that in animals affected by tick intoxication, the prevalence of fibrin, hemorrhage, and high–protein edema fluid in fatal tick paralysis strongly suggests either an inflammatory reaction or direct toxin effects on endothelial cells or type I pneumocytes. Such effects could contribute to greater vascular damage or enhanced permeability [22]. Lung slide was observed in all dogs included in the present study, both those affected by tick paralysis and those that were healthy. This finding may be attributed to the non–infectious nature of tick paralysis, as

opposed to disorders where lung slide is absent due to their etiology [26]. However, since acute lung injury may develop in dogs with tick paralysis, it may be important to investigate physiological patterns such as lung slide in evaluating the second phase of the inflammatory reaction, taking into account the duration of symptoms. In addition, alterations in the initial phase of the acute phase response that result in either exuberant or diminished fibrin deposition may give rise to early complications during convalescence, such as bleeding, thrombosis, systemic inflammatory response syndrome, or infection [27]. Therefore, the absence of normal findings on thoracic ultrasonography may convey critical clinical information regarding prognosis.

Normal lung tissue beneath the visceral pleural interface is obscured by shadowing and reverberation artifacts. Ribs appear bilaterally adjacent to the pleura, displaying smooth curvilinear echogenic interfaces with acoustic shadowing forming the gator sign (FIG. 2). These ribs are visualized at regular intervals while scanning the chest wall [28]. As reverberation artifacts, A–lines show up as horizontal, parallel lines at equal distances from one another. These lines are frequently observed in healthy individuals and indicate the presence of air or gas beneath the pleura. This air reflects ultrasound waves back to the probe, causing a back–and–forth movement of waves between the transducer and the air beneath the pleura (FIG. 3), thereby producing this artifact [25]. A–lines may be erased by B–lines or enhanced in the presence of pneumothorax [29]. False B–lines, such as Z–lines, appear perpendicular to the pleural line and can be confused with true B–lines. These lines, which are vertical and bundle–like in shape, originate from the pleural line. However, they are typically ill–defined, do not erase A–lines, and are not perfectly synchronous with respiratory movements [30]. Thoracic ultrasonography findings such as A–lines, Z–lines, and gator signs of the healthy dogs of the present study (FIGS. 4 and 5) were consistent with previously reported ultrasonographic findings of normal lung and were related to the air below the pleural line and the reflection of this air to ultrasound waves [31]. Previous studies have reported pulmonary parenchymal changes such as alveolar oedema,
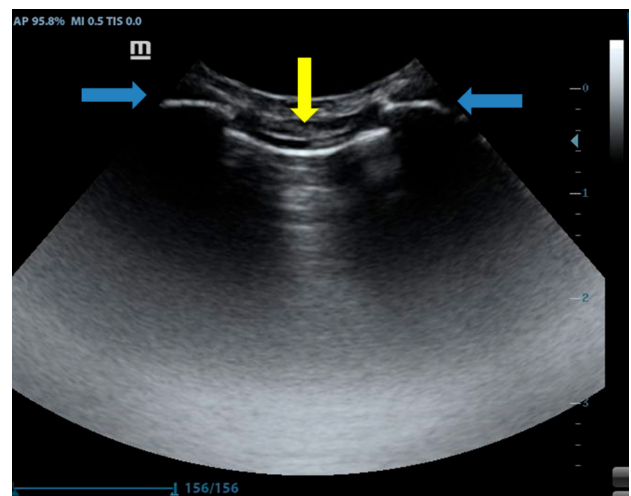


**FIGURE 2. Gator sign. The rounded rib heads resemble eyes (blue arrows), and the pulmonary–pleural interface looks like the bridge of a nose (yellow arrow), as if a partially submerged alligator is peering at the sonographer**
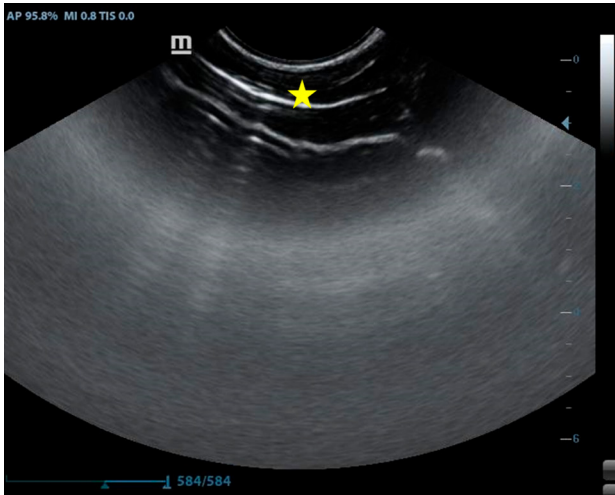
**FIGURE 3. Lung slide.** A back–and–forth movement of the visceral pleura in contact with the parietal pleura (yellow asteriks) is described as a shimmering or twinkling of the pleural line
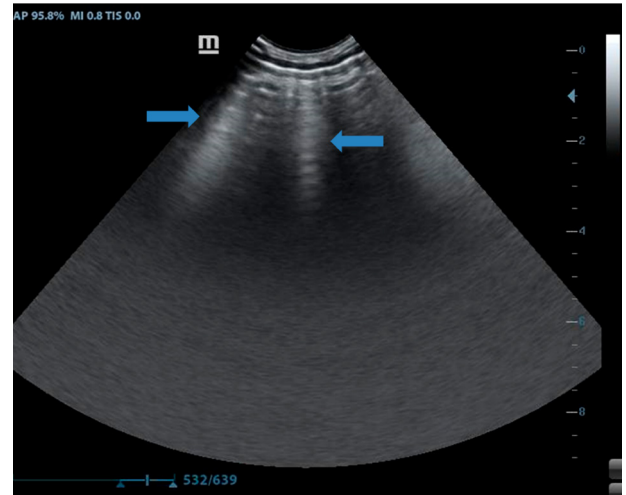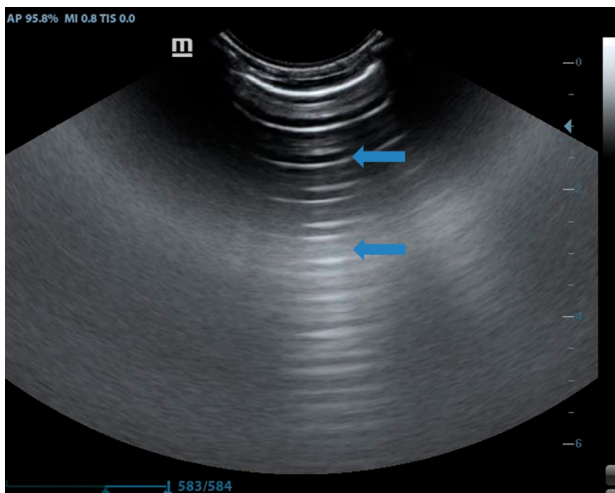


**FIGURE 5. Z–lines.** Vertical, bundle–like shaped lines emerging from the pleural line (blue arrows); however, these are not well defined, do not erase A–lines, and are not fully synchronized with respiratory movements

interstitial and alveolar congestion, and alveolar fibrin exudation in dogs with tick paralysis [22]. For this reason, the loss of A–lines determined in the dogs with tick paralysis (FIG. 6) may be related to the decrease in lung aeration resulting from parenchymal changes [32]. In addition, while areas with poor ventilation can be used to predict the development of atelectasis, it can also be interpreted as serving as a buffer zone between areas where ventilation is reduced and lung tissue collapses [33]. Thus, investigating the loss of A–line pattern may have prognostic importance in dogs with tick paralysis.

Unlike A–lines, B–lines are observed in interstitial–alveolar edema. They result from the repeated oscillation of ultrasound beams between air and fluid, producing a long, vertical hyperechoic artifact that starts at the pleural line and extends downward on the screen, moving in harmony with the pleural line during respiration [34]. The occurrence of these lines is attributed to small fluid
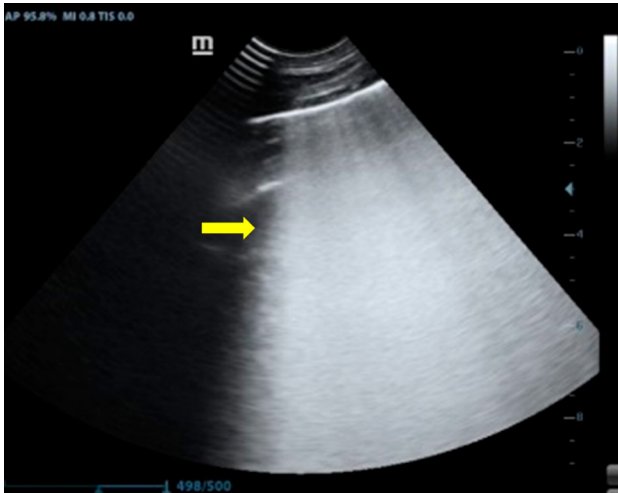


**FIGURE 6. Loss of A–lines.** Loss of A–lines indicating decreased or absence of aeration due to acute lung injury in the present case

accumulations in lung tissue, surrounded by air, creating a high impedance gradient. Both the number and width of these lines are related to the severity of the pathology. However, B–lines alone are inadequate for making a definitive diagnosis, as they indicate interstitial–alveolar fluid that can occur in both non–cardiogenic and cardiogenic pulmonary edema, as well as in conditions such as ARDS, pulmonary hemorrhage of various origins, pneumonia, lung contusion, neoplastic lung metastasis, or pulmonary fibrosis [35]. Assessing the number of B–lines is crucial, as an increase in lines during follow–up examinations indicates disease progression, while a decrease suggests that the treatment is effective. A single B–line may be physiological, however more indicate lung pathology [36]. In previous studies, a progressive reduction in respiratory rate and increase in inspiratory effort, hypoxaemia, marked hypercapnia, congestion and edema of the lung parenchyma and aspiration pneumonia were determined in dogs with tick paralysis [5, 14]. Findings such as confluent B–lines (FIG. 7) and pulmonary nodule (FIG. 8), as well as the observation



**FIGURE 4. A–lines.** Reverberation artifacts (blue arrows) that appear as horizontal, parallel lines equidistant from each other

FIGURE 7. Confluent B–lines. B–lines are fused with each other, occupying more than 50% of the image, defined as confluent B–lines (yellow arrow), indicating severe pulmonary edema.
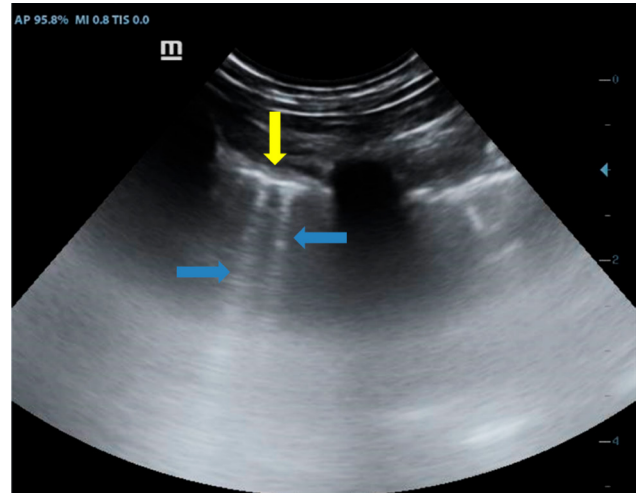


FIGURE 9. B–lines. Scattered B–lines (blue arrows), characterized by laser–like, vertical echogenic lines arising from the thickened irregular pleural line (yellow arrow) and extending to the bottom of the image, indicating pneumonia
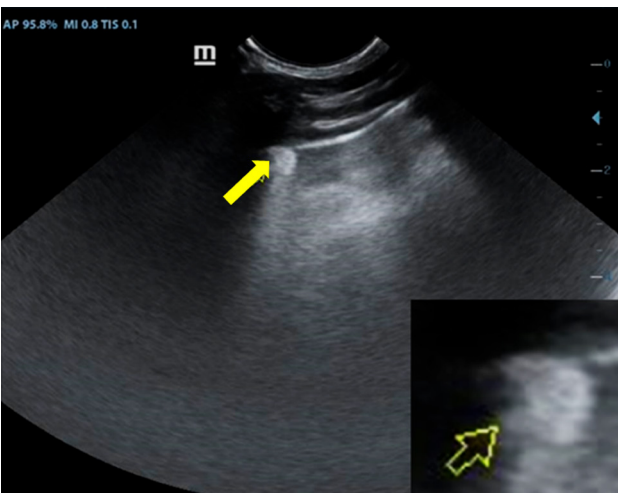


FIGURE 8. Pulmonary nodule. Yellow arrow(s) indicating a slightly hyperechoic pulmonary nodule with a regular rounded shape and well-defined margins (magnified thumbnail in the corner)
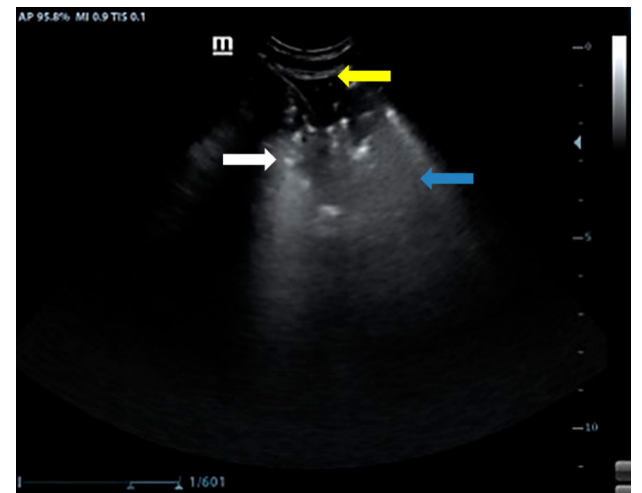


FIGURE 10. Consolidated lung area. A medium–sized area of consolidation, accompanied by minimal pleural effusion (yellow arrow), is defined by hypoechoic hepatized tissue (blue arrow). Within the consolidation, hyperechoic punctiform areas are observed and interpreted as air bronchograms (white arrow)

of B–lines > 3 (FIG. 9), may result from aspiration pneumonia and fibrin exudation [22], especially in tick–paralyzed dogs with megaesophagus and/or prominent crackling sounds on lung auscultation in the present study.

B–lines can be found not only in cardiogenic pulmonary edema but also in other types of non–cardiogenic inflammatory pulmonary edema, such as acute respiratory distress syndrome (ARDS). The distribution pattern of B–lines is instrumental in differentiating between cardiogenic pulmonary edema and ARDS: cardiogenic edema commonly shows a base–apex gradient, while ARDS tends to have an irregular and heterogeneous distribution [37]. In cases of chronic fibrosing interstitial diseases, key signs involve the presence of B–lines displaying particular features: a non–homogeneous distribution (dependent on the underlying pathology) and an irregularly thickened pleural line, often disrupted by small subpleural consolidations (FIG. 10), and B–lines that are thicker

and more irregular (FIG. 11) compared to those found in cardiogenic pulmonary edema [38]. Thus, when evaluating the characteristics of the B–lines in the present study, the abnormal thoracic patterns can be considered to originate from the pulmonary parenchyma and pleura [39]. Also, the presence of B–lines > 3 may confirm that the development of pulmonary parenchymal disease is one of the important complications of tick paralysis.

It was reported that tick neurotoxin has cardiotoxic effects [22]. Also, dogs with tick paralysis have been shown to have varying degrees of heart failure [6]. Myocardial dysfunction and subsequent left–sided congestive heart failure have been postulated as the causes of the pulmonary edema identified in dogs with tick paralysis [22]. Venous congestion, peribronchial fluid infiltration, and pulmonary edema due to heart failure result in a wet lung appearance on thoracic ultrasonography [40]. Pulmonary edema
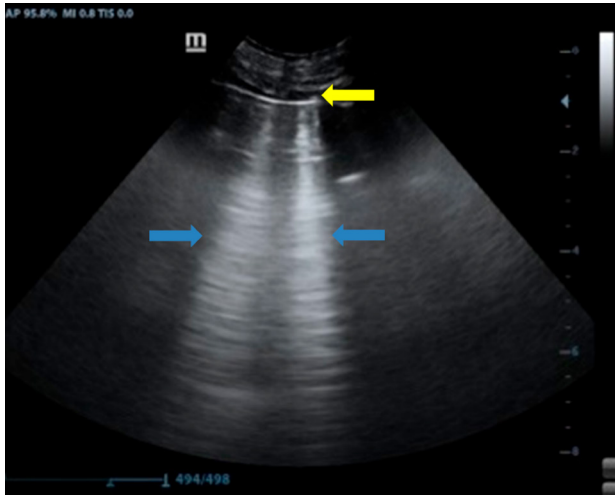
**FIGURE 11. Isolated B–line.** Visualization of two isolated B–lines (blue arrows) with a regular pleura (yellow arrow) in a single scan, which may be considered a normal finding horizontal

is a common finding in animals affected by tick paralysis. The pathophysiology of this process remains unclear, but it is an ongoing area of research interest. Previously, it was reported that pulmonary edema and congestion were observed in 9 out of 25 dogs euthanized due to tick paralysis [41]. In the present study, the detection of a wet lung on thoracic ultrasonography in dogs with tick paralysis ( FIG. 12) may indicate impending acute heart failure decompensation. Observing this pattern in dogs with tick paralysis may prompt lung decongestion therapy. Nevertheless, the risk of developing left–sided heart failure due to neuromuscular paralysis in dogs with tick paralysis should always be considered [6].

Benign pleural thickening resulting from fibrosis ranks as the second most common pleural abnormality following pleural effusion. Such thickening typically arises as a consequence of lung and pleural inflammation, with common causes encompassing
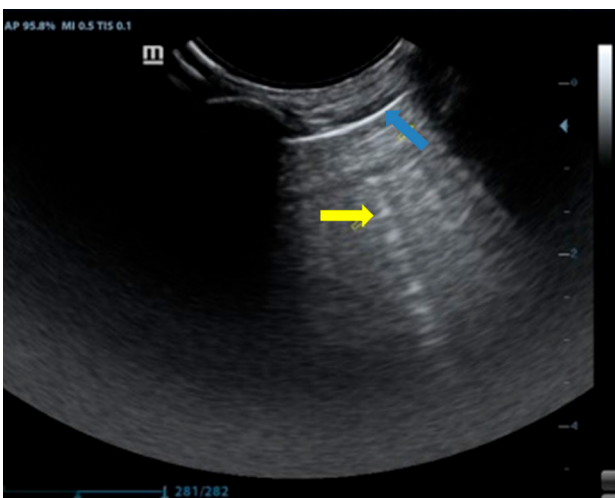


**FIGURE 12. Wet lung.** A wet lung appearance with a regular and thin pleura (blue arrow), along with increased, slightly blurred B–line (yellow arrow), which may be related to venous congestion in the present case

apical cap formation and pleural plaque development. Diffuse pleural thickening commonly arises after an episode of pleuritis, which leads to pleural fibrosis primarily involving the visceral pleura and causing adhesions to the parietal pleura [42]. Additionally, fibrotic lung diseases that affect the distal airways and pleura may also result in areas of pleural thickening or irregularity [43]. A previous study reported proteinaceous edema, along with mild to severe congestion, bronchopneumonia, and fibrin infiltration, in the lung histopathology of dogs with tick paralysis [5, 22]. In the present study, the pleural thickness of the dogs with tick paralysis (FIG. 13) was higher than that of the healthy dogs ($P<0.0001$). This finding may be associated with the previously mentioned presence of bronchopneumonia in dogs with tick paralysis, along with the development of fibrin exudation and fibrosis, especially considering the duration of symptoms [22, 43]. Although pulmonary fibrosis (FIG. 14) can be induced by various factors, the release of fibrosis–inducing factors such as IL-6, transforming growth factor β (TGF–β), and plasminogen activator inhibitor-1 (PAI-1) during the inflammatory phase of tick paralysis could contribute to this condition [44].
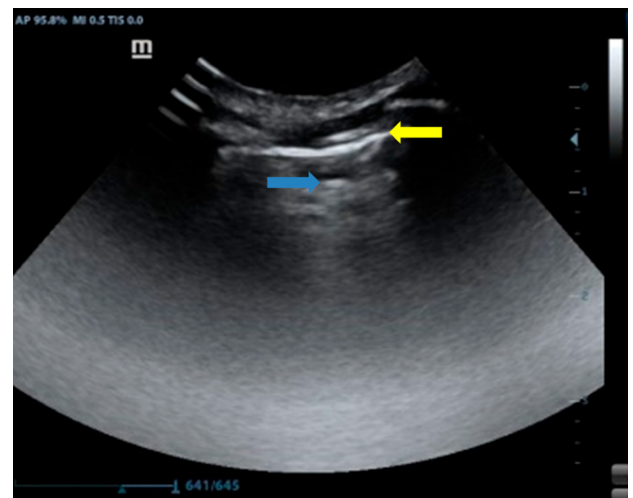


**FIGURE 13. Thickened pleural line.** A small focus of lung consolidation (blue arrow) is probably related to the inflammatory pneumonic process associated with ongoing tick paralysis, with thickened pleura (yellow arrow, 0.27 cm) that may indicate exudate

The limitations of this study include the absence of radiographic evaluation of the thorax, histopathological lung examinations, assessment of arterial blood gases or other functional measurements to evaluate lung ventilation and oxygenation of the tick–paralyzed dogs. Also, the lack of thoracic ultrasonographic examinations after recovery can also be considered a limitation. Moreover, a limitation is that the correlations between the evaluated laboratory parameters and abnormal thoracic ultrasonography findings were not investigated.
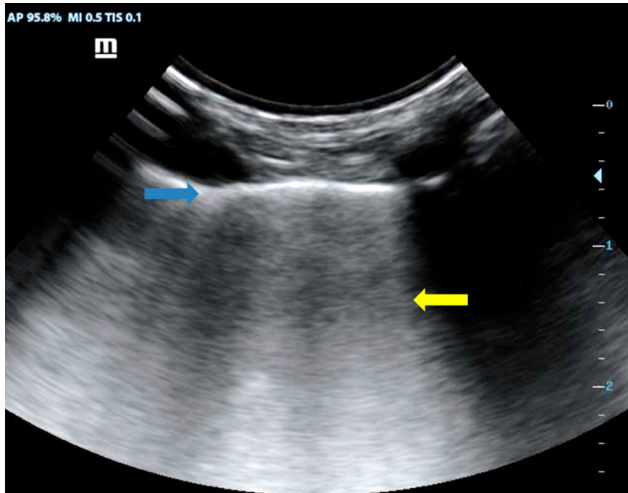
**FIGURE 14. Fibrosis. Mild fibrotic pulmonary involvement with multiple vertical comet–tail artifacts (yellow arrow) with an irregular, slightly thickened pleural line (blue arrow, 0.21 cm)**

## CONCLUSIONS

In this study, the most significant findings during the physical examination of dogs with tick paralysis were identified through lung auscultation. Fine crackle, polyphonic wheezing and pleural rub were the most prominent abnormal sounds. CBC results were within reference ranges. As a result of thoracic ultrasonography examination performed in 4 regions on both sides of the thorax, B–lines > 3, wet lung, pulmonary nodule, thickened pleura, confluent B–lines, consolidate, fibrosis and isolated B–line were determined as abnormal patterns in dogs with tick paralysis. Among these findings, it was thought that B–lines > 3 are due to possible pulmonary parenchymal damage; loss of A–lines, due to decreased aeration resulting from possible acute lung injury; pulmonary nodule and fibrosis formation might be due to bronchopneumonia and aspiration pneumonia in cases of tick paralysis. Additionally, wet lung was associated with a predisposition to develop lung congestion due to possible left heart failure in dogs with tick paralysis. In conclusion, recognition of thoracic ultrasonography findings in cases of tick paralysis may be helpful in identifying the presence and grading the extent of lung damage and deciding on the necessity of lung decongestion treatment. Evaluating these abnormal thoracic ultrasonography findings in conjunction with the results of radiographic, tomographic, and histopathological lung examinations, as well as arterial blood gas analyses and other functional measurements, may enhance the diagnostic and prognostic effectiveness of these patterns.

**Conflict of interest**

The authors declare there is no conflict of interest.

**BIBLIOGRAPHIC REFERENCES**

[1]  Pienaar R, Neitz AWH, Mans BJ. Tick paralysis: solving an enigma. Vet. Sci. [Internet]. 2018; 5(2):53. doi: https://doi.org/g82fh8

[2]  Padula AM. Tick paralysis of animals in Australia. In: Vogel CW, Seifert S, Tambourgi D, editors. Clinical toxinology in Australia, Europe, and Americas. Toxinology [Internet]. Dordrecht (Netherlands): Springer; 2018. p. 279-304. doi: https://doi.org/g82fh9

[3]  Holland CT. Asymmetrical focal neurological deficits in dogs and cats with naturally occurring tick paralysis (_Ixodes holocyclus_): 27 cases (1999-2006). Aust. Vet. J. [Internet]. 2008; 86(10):377-384. doi: https://doi.org/fgvxp4

[4]  Ruppin M, Sullivan S, Condon F, Perkins N, Lee L, Jeffcott LB, Dart AJ. Retrospective study of 103 presumed cases of tick (_Ixodes holocyclus_) envenomation in the horse. Aust. Vet. J. [Internet]. 2012; 90(5):175-180. doi: https://doi.org/g82fjb

[5]  Ilkiw JE, Turner DM, Howlett CR. Infestation in the dog by the paralysis tick _Ixodes holocyclus_ 1. Clinical and histological findings. Aust. Vet. J. [Internet]. 1987; 64(5):137-139. doi: https://doi.org/dfv4gh

[6]  Campbell F, Atwell R. Heart failure in dogs with tick paralysis caused by the Australian paralysis tick, _Ixodes holocyclus_. Int. J. Appl. Res. Vet. Med. [Internet]. 2003 [cited 12 Aug. 2024]; 1(2):148-162. Available in: https://goo.su/tVfJ

[7]  Atwell R. Laryngeal paresis caused by _I–holocyclus_. Aust. Vet. Pract. 2002; 32(1):41-41.

[8]  Nazerian P, Volpicelli G, Vanni S, Gigli C, Betti L, Bartolucci M, Zanobetti M, Ermini FR, Iannello C, Grifoni S. Accuracy of lung ultrasound for the diagnosis of consolidations when compared to chest computed tomography. Am. J. Emerg. Med. [Internet]. 2015; 33(5):620-625. doi: https://doi.org/f7b663

[9]  Touw HR, Tuinman PR, Gelissen HP, Lust E, Elbers PW. Lung ultrasound: routine practice for the next generation of internists. Neth. J. Med. [Internet]. 2015 [cited 12 Aug. 2024]; 73(3):100-107. PMID: 25852109. Available in: https://goo.su/qXtIgdq

[10]  Ward JL, Lisciandro GR, Keene BW, Tou SP, DeFrancesco TC. Accuracy of point–of–care lung ultrasonography for the diagnosis of cardiogenic pulmonary edema in dogs and cats with acute dyspnea. J. Am. Vet. Med. Assoc. [Internet]. 2017; 250(6):666-675. doi: https://doi.org/f9xq5r

[11]  Lichtenstein DA, Mezière GA. Relevance of lung ultrasound in the diagnosis of acute respiratory failure: the BLUE protocol. CHEST [Internet]. 2008; 134(1):117-125. doi: https://doi.org/cspcds

[12]  Koenig S, Mayo P, Volpicelli G, Millington SJ. Lung ultrasound scanning for respiratory failure in acutely ill patients: a review. CHEST [Internet]. 2020; 158(6):2511-2516. doi: https://doi.org/gnsr3p

[13]  Marx A, Glass JD, Sutter RW. Differential diagnosis of acute flaccid paralysis and its role in poliomyelitis surveillance. Epidemiol. Rev. [Internet]. 2000; 22(2):298-316. doi: https://doi.org/g82fjc

[14] Malik R, Farrow BR. Tick paralysis in North America and Australia. Vet. Clin. North. Am. Small. Anim. Pract. [Internet]. 1991; 21(1):157-171. doi: https://doi.org/g82fjd

[15] Martinez–Anton L, Marenda M, Firestone SM, Bushell RN, Child G, Hamilton AI, Long SN, Le Chevoir MAR. Investigation of the role of Campylobacter infection in suspected acute polyradiculoneuritis in dogs. J. Vet. Intern. Med. [Internet]. 2018; 32(1):352-360. doi: https://doi.org/gcvs6b

[16] Cuddon PA. Acquired canine peripheral neuropathies. Vet. Clin. North. Am. Small. Anim. Pract. [Internet]. 2002; 32(1):207-249. doi: https://doi.org/fwjdtf

[17] Musteata M, Nicolescu A, Solcan G, Deleanu C. The $^1$H NMR profile of healthy dog cerebrospinal fluid. PLoS One. [Internet]. 2013; 8(12):e81192. doi: https://doi.org/g82fjf

[18] Lisciandro GR, Fulton RM, Fosgate GT, Mann KA. Frequency and number of B–lines using a regionally based lung ultrasound examination in cats with radiographically normal lungs compared to cats with left–sided congestive heart failure: J. Vet. Emerg. Crit. Care [Internet]. 2017; 27(5):499-505. doi: https://doi.org/g82fjg

[19] Buda N, Kosiak W, Radzikowska E, Olszewski R, Jassem E, Grabczak EM, Pomiecko A, Piotrkowski J, Piskunowicz M, Sołtysiak M, Skoczyński S, Jaczewski G, Odrowska J, Skoczylas A, Wełnicki M, Wiśniewski J, Zamojska A, Polish Committee on Lung Ultrasound (PC–LUS) for POLLUS–IM. Polish recommendations for lung ultrasound in internal medicine (POLLUS–IM). J. Ultrason. [Internet]. 2018; 18(74):198-206. doi: https://doi.org/gfnpzj

[20] Ward JL, Lisciandro GR, Ware WA, Miles KG, Viall AK, DeFrancesco TC. Lung ultrasonography findings in dogs with various underlying causes of cough. J. Am. Vet. Med. Assoc. [Internet]. 2019; 255(5):574-583. doi: https://doi.org/gjnvmd

[21] Schull DN, O'Leary CA. The use of tick antitoxin serum and associated therapy for the treatment of dogs with *Ixodes holocyclus* toxicity. Aust. Vet. Pract. 2007; 37(3):90-97.

[22] Wang Y, Watters N, Jones E, Padula A, Leister E, Haworth M, Henning J, Allavena R. Pulmonary histopathology in cats and dogs with fatal tick paralysis. J. Comp. Pathol. [Internet]. 2022; 197:44-52. doi: https://doi.org/g82fjh

[23] Hecht S. Thorax. In: Penninck D, D'Anjou MA, editors. Atlas of small animal ultrasonography. Ames (Iowa, USA): Blackwell Publishing; 2008. p. 119-150.

[24] Lichtenstein DA. Lung ultrasound in the critically ill. Ann. Intensive. Care. [Internet]. 2014; 4(1). doi: https://doi.org/gcb3qq

[25] Saraogi A. Lung ultrasound: present and future. Lung India [Internet]. 2015; 32(3):250-257. doi: https://doi.org/gdwpg5

[26] Mooney ET, Rozanski EA, King RG, Sharp CR. Spontaneous pneumothorax in 35 cats (2001-2010). J. Feline Med. Surg. [Internet]. 2012; 14(6):384-391. doi: https://doi.org/f3xz8h

[27] Luyendyk JP, Schoenecker JG, Flick MJ. The multifaceted role of fibrinogen in tissue injury and inflammation. Blood [Internet]. 2019; 133(6):511-520. doi: https://doi.org/gj4jvh

[28] Lisciandro GR, Lagutchik MS, Mann KA, Voges AK, Fosgate GT, Tiller EG, Cabano NR, Bauer LD, Book BP. Evaluation of a thoracic focused assessment with sonography for trauma (TFAST) protocol to detect pneumothorax and concurrent thoracic injury in 145 traumatized dogs. J. Vet. Emerg. Crit. Care [Internet]. 2008; 18(3):258-269. doi: https://doi.org/dkmsjr

[29] Wongwaisaywan S, Suwannanon R, Sawatmongkorngul S, Kaewlai R. Emergency thoracic US: the essentials. Radiographics [Internet]. 2016; 36(3):640-659. doi: https://doi.org/f8ncv4

[30] Bouhemad B, Zhang M, Lu Q, Rouby JJ. Clinical review: bedside lung ultrasound in critical care practice. Crit. Care. [Internet]. 2007; 11(205). doi: https://doi.org/dnp4xw

[31] Volpicelli G. Sonographic diagnosis of pneumothorax. Intensive Care Med. [Internet]. 2011; 37(2):224-232. doi: https://doi.org/c48c93

[32] Via G, Lichtenstein D, Mojoli F, Rodi G, Neri L, Storti E, Klersy C, Iotti G, Braschi A. Whole lung lavage: a unique model for ultrasound assessment of lung aeration changes. Intensive Care Med. [Internet]. 2010; 36(6):999-1007. doi: https://doi.org/dxxkpw

[33] Reber A, Engberg G, Wegenius G, Hedenstierna G. Lung aeration: the effect of pre–oxygenation and hyperoxygenation during total intravenous anaesthesia. Anaesthesia. [Internet]. 1996; 51(8):733-737. doi: https://doi.org/cpxk44

[34] Touw HR, Parlevliet KL, Beerepoot M, Schober P, Vonk A, Twisk JW, Elbers PW, Boer C, Tuinman PR. Lung ultrasound compared with chest X–ray in diagnosing postoperative pulmonary complications following cardiothoracic surgery: a prospective observational study. Anaesthesia [Internet]. 2018; 73(8):946-954. doi: https://doi.org/gdxzkm

[35] Vezzosi T, Mannucci T, Pistoresi A, Toma F, Tognetti R, Zini E, Domenech O, Auriemma E, Citi S. Assessment of lung ultrasound B–lines in dogs with different stages of chronic valvular heart disease. J. Vet. Intern. Med. [Internet]. 2017; 31(3):700-704. doi: https://doi.org/f9xqw2

[36] Ward JL, Lisciandro GR, DeFrancesco TC. Distribution of alveolar–interstitial syndrome in dogs and cats with respiratory distress as assessed by lung ultrasound versus thoracic radiographs. J. Vet. Emerg. Crit. Care [Internet]. 2018; 28(5):415-428. doi: https://doi.org/g82fjj

[37] Patel CJ, Bhatt HB, Parikh SN, Jhaveri BN, Puranik JH. Bedside lung ultrasound in emergency protocol as a diagnostic tool in patients of acute respiratory distress presenting to emergency department. J. Emerg. Trauma Shock [Internet]. 2018; 11(2):125-129. doi: https://doi.org/gdr8x3

[38] Manolescu D, Oancea C, Timar B, Traila D, Malita D, Birsasteanu F, Tudorache V. Ultrasound mapping of lung changes in idiopathic pulmonary fibrosis. Clin. Respir. J. [Internet]. 2020; 14(1):54-63. doi: https://doi.org/g82fjk

[39] Gargani L. Lung ultrasound: a new tool for the cardiologist. Cardiovasc. Ultrasound [Internet]. 2011; 9(6). doi: https://doi.org/dxb4sf

[40] Raimondi F, Migliaro F, Sodano A, Umbaldo A, Romano A, Vallone G, Capasso L. Can neonatal lung ultrasound monitor fluid clearance and predict the need of respiratory support? Crit. Care [Internet]. 2012; 16(R220). doi: https://doi.org/g82fjm

[41] Webster RA. Tick paralysis 1 – pathophysiology, controversies and initial management. Continuing Veterinary Education, Proceedings No 411; 2014:91.

[42] Copley SJ, Wells AU, Rubens MB, Chabat F, Sheehan RE, Musk AW, Hansell DM. Functional consequences of pleural disease evaluated with chest radiography and CT. Radiology [Internet]. 2001; 220(1):237-243. doi: https://doi.org/g8brnf

[43] Chua F, Desai SR, Nicholson AG, Devaraj A, Renzoni E, Rice A, Wells AU. Pleuroparenchymal fibroelastosis: a review of clinical, radiological, and pathological characteristics. Ann. Am. Thorac. Soc. [Internet]. 2019; 16(11):1351-1359. doi: https://doi.org/gngnd6

[44] Leach HG, Chrobak I, Han R, Trojanowska M. Endothelial cells recruit macrophages and contribute to a fibrotic milieu in bleomycin lung injury. Am. J. Respir. Cell Mol. Biol. [Internet]. 2013; 49(6):1093-1101. doi: https://doi.org/f5j3qg